Hexairidium Clusters Supported on γ-Al_2O_3: Synthesis, Structure, and Catalytic Activity for Toluene Hydrogenation

A. Zhao and B. C. Gates*

Contribution from the Department of Chemical Engineering and Materials Science, University of California, Davis, California 95616

Received August 30, 1995[⊗]

Abstract: $[Ir_6(CO)_{15}]^{2-}$ was formed by surface-mediated synthesis on γ-Al_2O_3 powder by treatment of adsorbed $[Ir(CO)_2(acac)]$ in CO at 100 °C and 1 atm. The supported clusters were characterized by infrared and extended X-ray absorption fine structure (EXAFS) spectroscopies and by extraction into solution by cation metathesis. Treatment of γ-Al_2O_3-supported $[Ir_6(CO)_{15}]^{2-}$ in He at 300 °C led to decarbonylation without disruption of the cluster frame, giving Ir_6/γ-Al_2O_3, as indicated by EXAFS data determining a first-shell Ir−Ir coordination number of 4.05 ± 0.07 (where the error bounds represent precision, not accuracy), matching that of the supported $[Ir_6(CO)_{15}]^{2-}$, with a first-shell Ir−Ir coordination number of 4.07 ± 0.03. The supported Ir_6 clusters were found to be catalytically active for toluene hydrogenation at temperatures in the range of 60−100 °C; the turnover frequency at 60 °C with a toluene partial pressure of 50 Torr and a H_2 partial pressure of 710 Torr was 1.7×10^{-3} s^{-1}. The catalyst was stable in operation in a flow reactor, and consistent with this observation, EXAFS results for the used catalyst indicated that the nuclearity of the supported Ir_6 clusters was essentially unchanged during catalysis. The γ-Al_2O_3-supported Ir_6 catalyst is an order of magnitude less active (per total Ir atom) for toluene hydrogenation than a catalyst consisting of small aggregates of iridium (with an average of about 50 atoms each) supported on γ-Al_2O_3. Because toluene hydrogenation is known to be a structure-insensitive catalytic reaction, the data suggest that the concept of structure insensitivity in catalysis does not extend to clusters as small as Ir_6. However, the relatively low activity of the Ir_6 clusters may be more an indication of an effect of the support as a ligand changing the electronic properties of the iridium in the cluster than an effect of the cluster size.

Introduction

Supported metals are among the most important industrial catalysts, usually consisting of metallic particles dispersed on metal oxide supports.[1−5] The recent industrial application of platinum clusters, typically 4−5 atoms in nuclearity,[6] in LTL zeolite as catalysts for naphtha dehydrocyclization[7,8] has led to heightened interest in extremely small clusters on supports and their catalytic properties.[9] Only a few catalysts consisting of structurally well-defined metal clusters on supports have been reported.[9,10] Following a recent communication of catalytic results for such clusters,[10] we now report (1) the synthesis of $[Ir_6(CO)_{15}]^{2-}$ on γ-Al_2O_3, (2) its decarbonylation to give supported Ir_6, (3) the structural characterization of the supported clusters, and (4) the catalytic performance of Ir_6 for toluene hydrogenation.

Results

Evidence of Formation of $[Ir_6(CO)_{15}]^{2-}$ on γ-Al_2O_3. A. Infrared Spectroscopy and Extraction. $[Ir(CO)_2(acac)]$ in *n*-hexane solution was brought in contact with the uncalcined γ-Al_2O_3 support. After removal of the solvent by evacuation, the solid was beige and had an infrared spectrum with two strong ν_{CO} bands, at 2075 and 1994 cm^{-1}, indicating an iridium dicarbonyl species.[11] This is formulated as $Ir(I)(CO)_2/\gamma$-Al_2O_3.[11]

Treatment of $Ir(I)(CO)_2/\gamma$-Al_2O_3 in flowing CO at 100 °C for 10 h led to an orange-brown solid with an infrared spectrum (ν_{CO}: 2067 sh, 2040 m, 2010 vs, 1837 w cm^{-1}, Figure 1)[12] closely resembling that of $[Ir_6(CO)_{15}]^{2-}$ supported on MgO powder (ν_{CO}: 2060 m, 2012 vs, 1832 w cm^{-1}).[13] Extraction of the surface species with [PPN][Cl] [PPN is bis(triphenylphosphine)nitrogen(1+)] in freshly distilled THF (tetrahydrofuran) resulted in a red-brown solution, the infrared spectrum of which is shown in Figure 2. The ν_{CO} bands at 2030 sh, 1983 s, 1979 s, 1922 w, and 1772 m cm^{-1} match those reported for $[PPN]_2[Ir_6(CO)_{15}]$ in THF.[14] This result is consistent with the inference that $[Ir_6(CO)_{15}]^{2-}$ formed on the surface of γ-Al_2O_3 and was extracted into solution by cation metathesis.

The weak ν_{CO} bands at 2042 and 1957 cm^{-1} characterizing the extract solution (Figure 2) indicate the presence of a small amount of unconverted mononuclear iridium carbonyl species that were presumably extracted from the surface along with $[Ir_6(CO)_{15}]^{2-}$.[15] Another weak ν_{CO} band was observed for the extract solution, at 2015 cm^{-1}. This band shows that a small amount of another (unidentified) iridium carbonyl was extracted, possibly $[HIr_4(CO)_{11}]^-$.[16]

* To whom correspondence should be addressed.

[⊗] Abstract published in *Advance ACS Abstracts,* March 1, 1996.

(1) Anderson, J. R. *Structure of Metallic Catalysts*; Academic Press: New York, 1975.
(2) Boudart, M. *J. Mol. Catal.* **1985**, *30*, 27.
(3) Sinfelt, J. H. *Bimetallic Catalysts: Discoveries, Concepts, and Applications;* Exxon Monograph; Wiley: New York, 1983.
(4) Boudart, M. *Adv. Catal.* **1969**, *20*, 153.
(5) Boudart, M.; Djéga-Mariadassou, G. *Kinetics of Heterogeneous Catalytic Reactions;* Princeton University Press: Princeton, NJ, 1984.
(6) Vaarkamp, M.; Grondelle, J. V.; Miller, J. T.; Sajkowski, D. J.; Modica, F. S.; Lane, G. S.; Gates, B. C.; Koningsberger, D. C. *Catal. Lett.* **1990**, *6*, 369.
(7) *Oil Gas J.* **1992**, *190*, 29.
(8) Rotman, D. *Chem. Week* **1992**, *150*, 8.
(9) Gates, B. C. *Chem. Rev.* **1995**, *95*, 511.
(10) Xu, Z.; Xiao, F.-S.; Purnell, S. K.; Alexeev, O.; Kawi, S.; Deutsch, S. E.; Gates, B. C. *Nature (London)* **1994**, *372*, 346.
(11) Kawi, S.; Chang, J.-R.; Gates, B. C. *J. Phys. Chem.* **1993**, *97*, 5375.
(12) Infrared evidence of formation of surface intermediates: when the temperature was ramped to 100 °C at a rate of 5 °C/min after exposure of the sample to CO at 1 atm, the ν_{CO} band at 1994 cm^{-1} decreased in intensity and shifted to 1997 cm^{-1}; the band at 2075 cm^{-1} shifted to 2071 cm^{-1}. A new band appeared at 2036 cm^{-1} and increased in intensity.
(13) Maloney, S. D.; Kelley, M. J.; Koningsberger, D. C.; Gates, B. C. *J. Phys. Chem.* **1991**, *95*, 9406.
(14) Gladfelter, W. L. Personal communication, 1991.
(15) Kawi, S.; Gates, B. C. *Inorg. Chem.* **1992**, *31*, 2939.

0002-7863/96/1518-2458$12.00/0

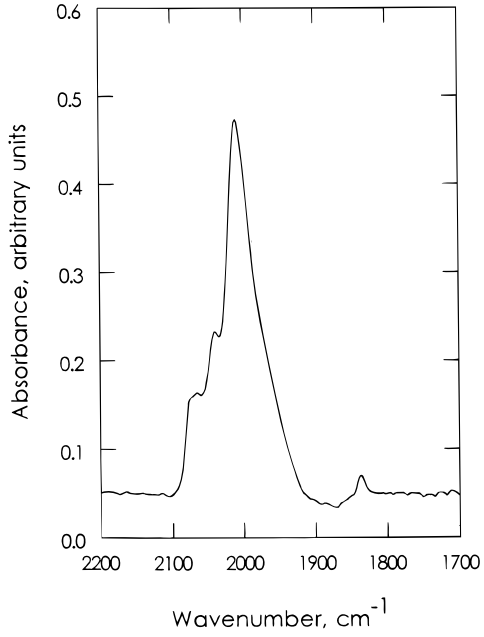

Figure 1. Infrared spectrum of the species prepared by adsorption of $[Ir(CO)_2(acac)]$ on uncalcined γ-Al_2O_3 followed by treatment in CO at 1 atm and 100 °C for 10 h.

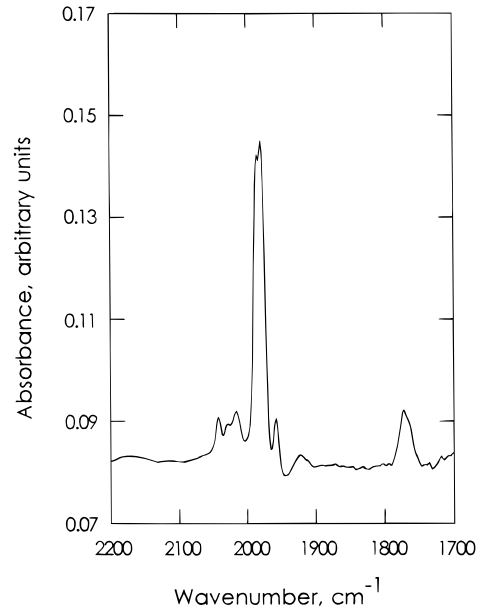

Figure 2. Infrared spectrum of the extract solution formed by bringing the sample represented by the spectrum in Figure 1 in contact with [PPN][Cl] in THF.

B. Mass Spectrometry. Analysis of the extract solution by fast atom bombardment mass spectrometry in the negative ion mode provided a confirmation that $[Ir_6(CO)_{15}]^{2-}$ was present in the extract solution. The mass spectrum included a peak at *m/z* 1577 corresponding to the dianion $[Ir_6(CO)_{15}]^{2-}$, which was accompanied by numerous other peaks, including some consistent with loss of carbonyl ligands and fragmentation of the metal framework.

C. EXAFS Spectroscopy. The raw EXAFS data characterizing the carbonylated sample, shown in Figure 3A, are an average of results for six scans. The data show oscillations up to a value of *k*, the wave vector, of about 17.5 $Å^{-1}$, with the standard deviation in the EXAFS function being less than 0.0005. The EXAFS analysis[17] was done with experimentally determined reference files described in the section below entitled EXAFS Reference Data; the methods of data analysis are summarized below in the section entitled EXAFS Data Analysis.

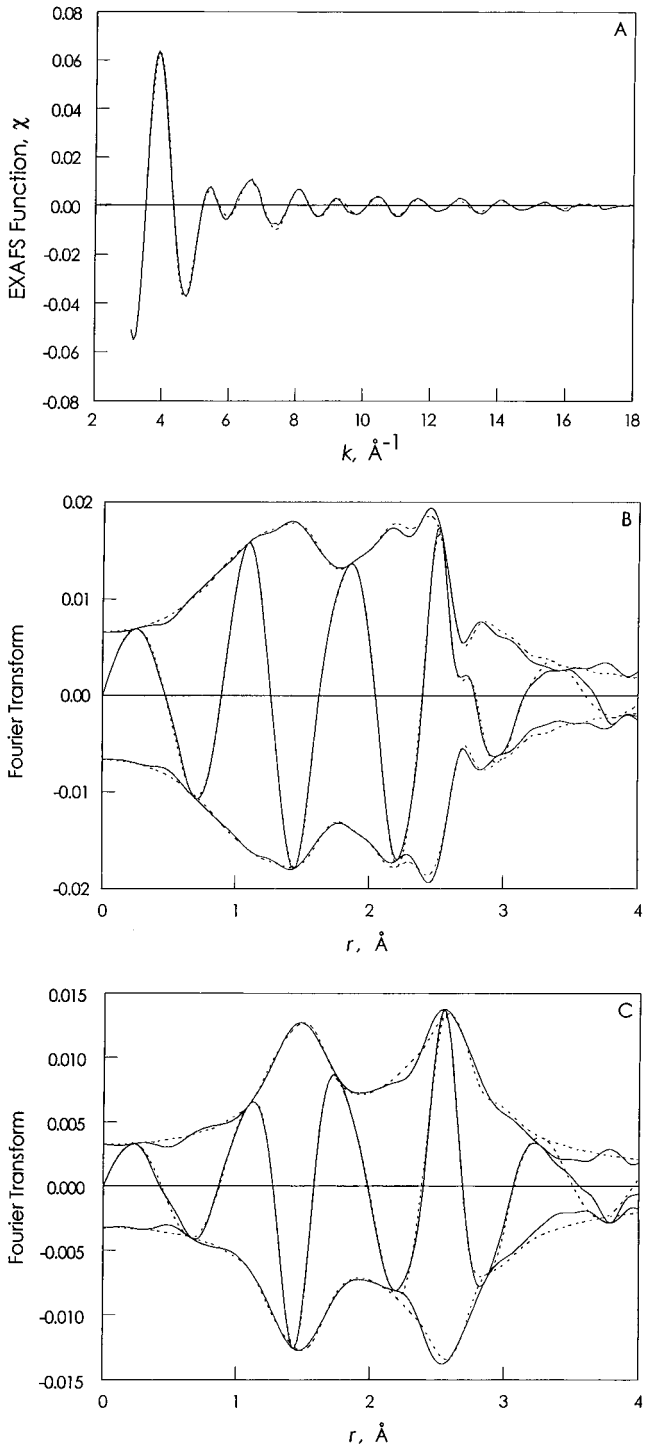

Figure 3. Results of EXAFS data analysis characterizing γ-Al_2O_3-supported $[Ir_6(CO)_{15}]^{2-}$: (A) raw EXAFS function (solid line) and sum of the calculated Ir−Ir + Ir−C_t + Ir−C_b + Ir−O* + Ir−$O_{support}$ + Ir−Al contributions (dashed line); (B) imaginary part and magnitude of Fourier transform (unweighted; Δk = 3.50−16.45 $Å^{-1}$) of raw EXAFS function and sum of the calculated Ir−Ir + Ir−C_t + Ir−C_b + Ir−O* + Ir−$O_{support}$ + Ir−Al contributions (dashed line); (C) residual spectrum illustrating the contributions of carbonyl ligands: imaginary part and magnitude of Fourier transform (unweighted; Δk = 3.50−16.45 $Å^{-1}$) of raw EXAFS data minus calculated Ir−Ir + Ir−$O_{support}$ + Ir−Al contributions (solid line) and calculated Ir−C_t + Ir−C_b + Ir−O* contributions (dashed line).

(16) Angoletta, M.; Malatesta, L.; Caglio, G. *J. Organomet. Chem.* **1975,** *94,* 99.

Table 1. EXAFS Results Characterizing γ-Al_2O_3-Supported $[Ir_6(CO)_{15}]^{2-}$ Prepared from $[Ir(CO)_2(acac)]$ Supported on γ-Al_2O_3 after Treatment in CO at 100 °C and 1 atm for 10 h[a]

shell	coordination no., N	distance, r, Å	$10^3 \times$ Debye−Waller factor, $\Delta\sigma^2$, Å^2	inner potential corr, ΔE_0, eV	EXAFS ref
Ir−Ir	4.07 ± 0.03	2.751 ± 0.000	2.10 ± 0.04	4.54 ± 0.10	Pt−Pt
Ir−CO					
Ir−C_t	2.13 ± 0.04	1.874 ± 0.002	0.74 ± 0.21	4.27 ± 0.21	Ir−C
Ir−C_b	1.17 ± 0.06	2.191 ± 0.004	1.03 ± 0.57	17.53 ± 0.53	Ir−C
Ir−O*	2.03 ± 0.01	2.985 ± 0.001	0.92 ± 0.09	−1.26 ± 0.04	Ir−O*
Ir−$O_{support}$	0.47 ± 0.06	2.150 ± 0.009	0.50 ± 0.57	−5.02 ± 0.39	Pt−O
Ir−Al	0.56 ± 0.01	1.543 ± 0.001	5.76 ± 0.23	3.82 ± 0.32	Ir−Al

[a] The error bounds stated here were obtained from the statistical analysis of the data; they indicate the precisions, not accuracies. The subscripts b and t refer to bridging and terminal, respectively.

In addition to the Ir−Ir, Ir−C, Ir−O* (where O* refers to carbonyl oxygen), and Ir−$O_{support}$ (where $O_{support}$ refers to oxygen of the support) contributions, a small contribution, tentatively associated with Al of the support, was included to give good agreement between the fit and the data. The structural parameters are summarized in Table 1, and the comparisons of the data and the fit, both in k space and in r space, are shown in Figures 3A and 3B. The residual spectrum determined by subtracting the sum of the Ir−Ir + Ir−$O_{support}$ + Ir−Al contributions from the raw EXAFS data (which gives evidence of the carbonyl ligands) is shown in Figure 3C.

The number of parameters used to fit the data in this main-shell analysis is 24; the statistically justified number is approximately 42, estimated from the Nyquist theorem,[18] $n = (2\Delta k \Delta r/\pi) + 1$, where Δk and Δr respectively are the k and r ranges used in the data fitting ($\Delta k = 12.95$ Å^{-1}; $\Delta r = 5$ Å). Estimates of the standard deviations in the EXAFS parameters were determined with the XDAP software[19] (calculated from the covariance matrix including the statistical errors of the experimental points), as summarized in Table 1.

Influence of Water on the Formation of γ-Al_2O_3-Supported $[Ir_6(CO)_{15}]^{2-}$. The same carbonylation process was also carried out with samples prepared from $[Ir(CO)_2(acac)]$ adsorbed on γ-Al_2O_3 that had been calcined at 100, 300, or 400 °C. Treatment of each sample in CO at 100 °C for 10 h (the standard treatment conditions) led to the infrared spectra shown in Figure 4.

The spectrum of the carbonylated species supported on 100 °C-calcined γ-Al_2O_3 had ν_{CO} bands in the same positions (2067 s, 2040 ms, 2010 s, and 1837 vw cm^{-1}) as were observed for $[Ir_6(CO)_{15}]^{2-}$ on uncalcined γ-Al_2O_3, but with different intensities, indicating an incomplete conversion of mononuclear $[Ir(CO)_2(acac)]$ into hexairidium carbonyls on the surface of γ-Al_2O_3.

The infrared spectrum of the carbonylated species formed on γ-Al_2O_3 calcined at 300 °C had ν_{CO} bands at 2071 s, 2036 w, and 2002 sh cm^{-1}. Extraction of the surface species by [PPN][Cl] in freshly distilled THF gave an infrared spectrum suggesting the presence of $[Ir_4(CO)_{12}]$ (ν_{CO}: 2067 s, 2029 m),[15,20] $[HIr_4(CO)_{11}]^-$ (ν_{CO}: 2015 s, 1800 w),[16] $[Ir_4(CO)_{11}Cl]^-$ (ν_{CO}: 2043 s, 2003 s, 1833 m),[14,21,22] $[Ir_6(CO)_{15}]^{2-}$ (ν_{CO}: 1985 w, 1976 w, 1779 w),[14] and $[Ir(CO)_2Cl_2]^-$ (ν_{CO}: 2043 s, 1957 s)[15] in the solution. The results suggest that tetrairidium carbonyl clusters, either neutral or anionic, were the predominant species formed on the surface of γ-Al_2O_3 and that, in addition, there were unconverted mononuclear iridium dicarbonyl precursors and small amounts of hexairidium carbonyl clusters. Thus the results show that the chemistry occurring on the surface of γ-Al_2O_3 calcined at 300 °C is different from that occurring on the surface of uncalcined γ-Al_2O_3.

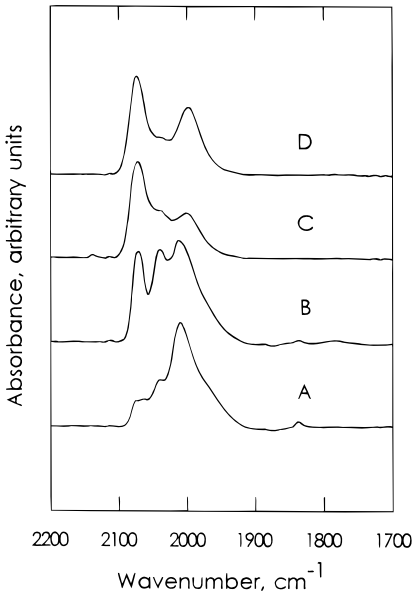

Figure 4. Infrared spectra of samples prepared by adsorption of $[Ir(CO)_2(acac)]$ on γ-Al_2O_3 followed by treatment in CO at 1 atm and 100 °C for 10 h; the γ-Al_2O_3 support was calcined at different temperatures T: (A) uncalcined; (B) $T = 100$ °C; (C) $T = 300$ °C; (D) $T = 400$ °C.

The infrared spectrum of the carbonylated species (ν_{CO}: 2075s, 2036vw, 1994s cm^{-1}) prepared from γ-Al_2O_3 that had been calcined at 400 °C was virtually the same as that of the original iridium dicarbonyl species (ν_{CO}: 2075 s, 1994 s cm^{-1}), except that the intensity of the ν_{CO} band at 1994 cm^{-1} had decreased slightly, indicating that the carbonylation process had taken place to only a small extent on the surface that had been calcined at 400 °C and thus was more highly dehydroxylated than the samples calcined at lower temperatures.[23]

Reductive Carbonylation−Oxidative Fragmentation Cycle. Overnight exposure of γ-Al_2O_3-supported $[Ir_6(CO)_{15}]^{2-}$ to air led to a violet-blue sample, the infrared spectrum of which is shown in Figure 5B. The ν_{CO} bands at 2075 s and 1994 s cm^{-1} are the same as those characteristic of the mononuclear iridium dicarbonyls adsorbed on γ-Al_2O_3; the ν_{CO} bands at 2062 sh, 2040 w, and 2023 m cm^{-1} match almost exactly the infrared spectrum of $[Ir_4(CO)_{12}]$ adsorbed on γ-Al_2O_3 (ν_{CO}: 2062 s, 2040 m, 2024 s, 2003 m).[11] Thus these data indicate that the

(17) Koningsberger, D. C. In *Synchrotron Techniques in Interfacial Electrochemistry*; Melendres, C. A., Tadjeddine, A., Eds.; Kluwer: Dordrecht, The Netherlands, 1994; p 181.

(18) Crozier, E. D.; Rehr, J. J.; Ingalls, R. In *X-ray Absorption: Principles, Applications, Techniques of EXAFS, SEXAFS, and XANES;* Koningsberger, D. C., Prins, R., Eds.; Wiley: New York, 1988; p 395.

(19) Vaarkamp, M.; Linders, J. C.; Koningsberger, D. C. *Physica B* **1995**, *209*, 159.

(20) Adams, D. M.; Taylor, I. D. *J. Chem. Soc., Faraday Trans. 2* **1982**, *78*, 1573.

(21) Chini, P.; Ciani, G.; Garlaschelli, L.; Manassero, M.; Martinengo, S.; Sironi, A.; Canziani, F. *J. Organomet. Chem.* **1978**, *152*, C35.

(22) Della Pergola, R.; Garlaschelli, L.; Martinengo, S. *J. Organomet. Chem.* **1987**, *331*, 271.

(23) Knözinger, H.; Ratnasamy, P. *Catal. Rev.—Sci. Eng.* **1978**, *17*, 31.

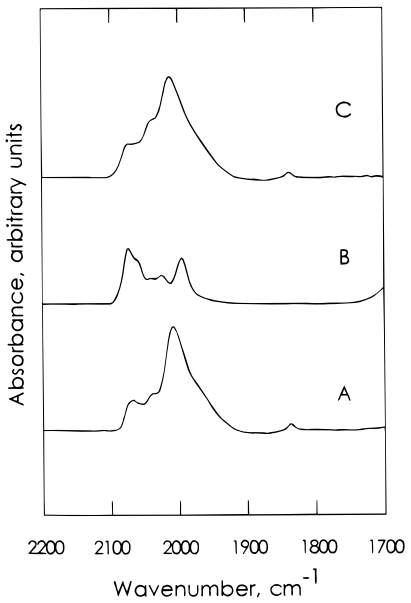

Figure 5. Infrared spectra characterizing the reactivity of γ-Al_2O_3-supported $[Ir_6(CO)_{15}]^{2-}$: (A) γ-Al_2O_3-supported $[Ir_6(CO)_{15}]^{2-}$; (B) sample after exposure to air overnight; (C) after subsequent CO treatment of sample at 100 °C for 10 h.

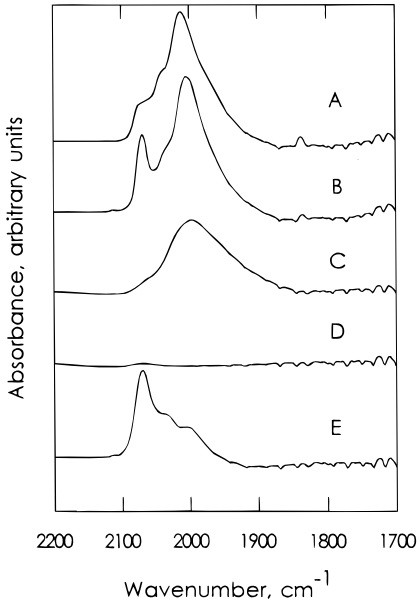

Figure 6. Infrared spectra characterizing the decarbonylation of γ-Al_2O_3-supported $[Ir_6(CO)_{15}]^{2-}$ by treatment in He at 1 atm as the temperature was ramped up to 300 °C at 3 °C/min, followed by recarbonylation of the iridium clusters: (A) γ-Al_2O_3-supported $[Ir_6(CO)_{15}]^{2-}$; (B) sample in He at 100 °C; (C) sample in He at 280 °C; (D) sample after treatment in He at 300 °C for 2 h; (E) sample after subsequent CO treatment at 100 °C for 3 h.

hexairidium carbonyl on γ-Al_2O_3 was oxidatively fragmented.

Treatment of the mixture of supported iridium carbonyls formed by oxidation in a flow reactor with CO at 1 atm and room temperature immediately brought the color back to beige, then orange-pink. Continuation of the CO treatment at 100 °C for 10 h led to the infrared spectrum shown in Figure 5C, which is the same as that of $[Ir_6(CO)_{15}]^{2-}$ supported on γ-Al_2O_3 (Figure 5A). Thus we conclude that $[Ir_6(CO)_{15}]^{2-}$ was reversibly fragmented and reconstructed on the surface by successive oxidation and carbonylation treatments. The surface species are robust, the cycle is repeatable, and the treatment conditions are mild. Thus samples that might be inadvertently contaminated with air can be reconverted into metal carbonyl clusters.

Infrared Spectra Characterizing the Decarbonylation of $[Ir_6(CO)_{15}]^{2-}$ on γ-Al_2O_3. Treatment of the supported $[Ir_6(CO)_{15}]^{2-}$ in flowing He at 1 atm as the temperature was ramped up at 3 °C/min to 300 °C led to a series of changes in the infrared spectra of the surface species (Figure 6). When the temperature had reached 100 °C, the ν_{CO} band at 2010 cm^{-1} had shifted to lower frequency, 2002 cm^{-1}, but remained the same intensity; the intensity of the ν_{CO} band at 2068 cm^{-1} increased; and the bridging ν_{CO} band at 1836 cm^{-1} was reduced in intensity. When the temperature had reached 280 °C, the ν_{CO} bands at 2068 and 1836 cm^{-1} had disappeared, and the ν_{CO} band at 2002 cm^{-1} was broadened and reduced in intensity. Continuation of the treatment in CO at 300 °C for 2 h led to the complete disappearance of ν_{CO} bands in the spectrum.

Recarbonylation of the Decarbonylated Iridium Clusters. CO at 1 atm was introduced into the room-temperature cell containing the decarbonylated clusters on γ-Al_2O_3 that had been formed by treatment of supported $[Ir_6(CO)_{15}]^{2-}$ in He at 300 °C. As the temperature increased to 100 °C at a rate of 5 °C/min, ν_{CO} bands appeared at 2070 s, 2035 sh, and 2004 sh cm^{-1} (Figure 6E). The spectrum did not change after further treatment of the sample at 100 °C for 3 h. The spectrum of $[Ir_6(CO)_{15}]^{2-}$ on γ-Al_2O_3 did not reappear. Rather, the spectrum almost matches that of the mixture of carbonylated species (mainly tetrairidium carbonyls and mononuclear iridium carbonyls) that had been formed on γ-Al_2O_3 calcined at 300 °C (2071 s, 2036 w, and 2002 sh cm^{-1}, Figure 4C). The results suggest that the carbonylated species formed on the surface depend primarily on the concentration of surface hydroxyl groups, which is determined by the temperature of treatment (provided that there are enough surface hydroxyl groups to influence the reactivity); formation of metal crystallites by sintering is likely if the surface is largely dehydroxylated.[24]

Characterization of Decarbonylated Iridium Clusters by EXAFS Spectroscopy. The EXAFS data characterizing the decarbonylated iridium clusters formed by thermal treatment of $[Ir_6(CO)_{15}]^{2-}$ in He at 300 °C for 2 h were analyzed as described in the section entitled EXAFS Data Analysis. The normalized EXAFS function for the decarbonylated clusters was obtained from the average of the X-ray absorption spectra from six scans, with the standard deviations in the EXAFS function being less than 0.0005 over the whole range of *k* space; the raw EXAFS data show oscillations up to *k* equal to about 17 $Å^{-1}$ (Figure 7A).

The EXAFS data analysis results (Table 2) confirm the presence of an Ir−Ir contribution and metal-support contributions, including Ir−O_s and Ir−O_l (where the subscripts s and l refer to short and long, respectively); the Ir−O_s distance is a bonding distance, but the Ir−O_l distance is too long to be a bonding distance. In addition, a small Ir−Al contribution was included in the fitting. The structural parameters with standard deviations are summarized in Table 2. The number of parameters used to fit the data in this main-shell analysis is 16; the statistically justified number, calculated from the Nyquist theorem ($\Delta k = 12.5$ $Å^{-1}$, $\Delta r = 5$ Å), is approximately 41. To show the goodness of fit for both high-*Z* (Ir) and low-*Z* (O, Al) contributions, the raw data are compared with the fit in *k* space and in *r* space (Figures 7A and 7B); the agreement is good.

The Ir−Ir coordination number of 4.05 ± 0.07 is consistent with the presence of octahedral Ir_6 and the postulate that the octahedral metal frame of $[Ir_6(CO)_{15}]^{2-}$ remained intact after decarbonylation. The decarbonylated iridium cluster is thus represented as Ir_6/γ-Al_2O_3, where it is implied that the cluster has an octahedral frame.

(24) Triantafillou, N. D.; Gates, B. C. *J. Phys. Chem.* **1994**, *98*, 8431.

Table 2. EXAFS Results Characterizing the Iridium Clusters Formed by Decarbonylation of $[Ir_6(CO)_{15}]^{2-}$ on γ-Al_2O_3 in He at 300 °C[a]

shell	coordination no., N	distance, r, Å	$10^3 \times$ Debye−Waller factor, $\Delta\sigma^2$, Å^2	inner potential corr, ΔE_0, eV	EXAFS ref
Ir−Ir	4.05 ± 0.07	2.704 ± 0.001	5.83 ± 0.11	−2.70 ± 0.16	Pt−Pt
Ir−$O_{support}$					
Ir−O_s	0.83 ± 0.01	2.227 ± 0.002	2.27 ± 0.31	−19.51 ± 0.16	Pt−O
Ir−O_l	0.61 ± 0.02	2.706 ± 0.002	−6.94 ± 0.11	−6.95 ± 0.26	Pt−O
Ir−Al	0.58 ± 0.02	1.554 ± 0.002	12.51 ± 0.37	14.58 ± 0.42	Ir−Al

[a] The error bounds stated here were obtained from the statistical analysis of the data; they indicate the precisions, not accuracies.

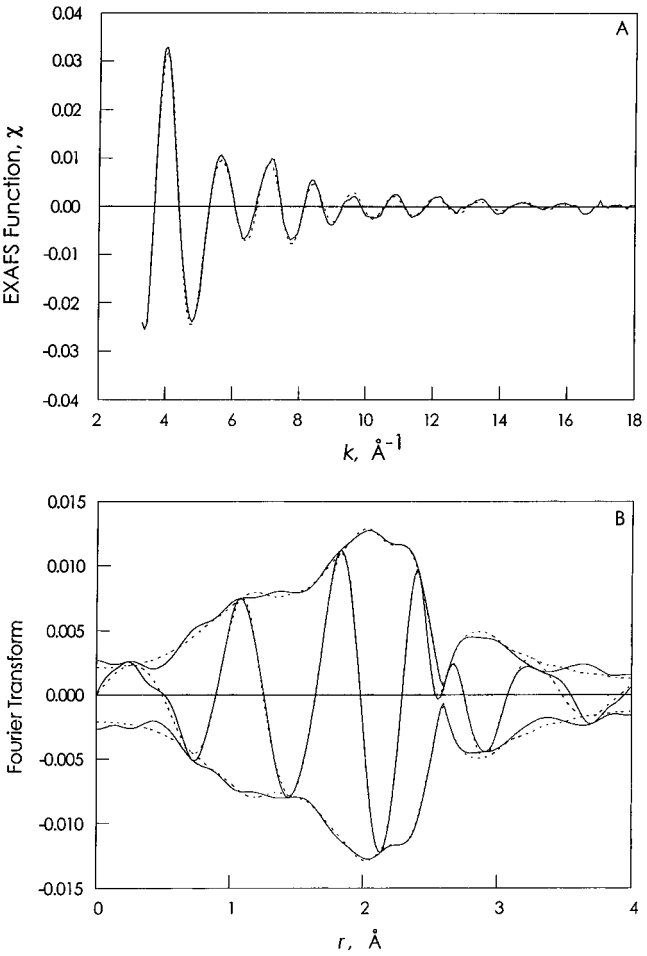

Figure 7. Results of EXAFS analysis characterizing γ-Al_2O_3-supported iridium clusters formed by decarbonylation of γ-Al_2O_3-supported $[Ir_6(CO)_{15}]^{2-}$ in He at 300 °C for 2 h: (A) raw EXAFS function (solid line) and sum of the calculated Ir−Ir + Ir−O_s + Ir−O_l + Ir−Al contributions (dashed line); (B) imaginary part and magnitude of Fourier transform (unweighted; $\Delta k = 3.68-16.26$ Å^{-1}) of raw EXAFS function (solid line) and sum of the calculated Ir−Ir + Ir−O_s + Ir−O_l + Ir−Al contributions (dashed line).

Toluene Hydrogenation Catalyzed by γ-Al_2O_3-Supported Iridium Catalysts. A. Ir_6/γ-Al_2O_3. Toluene hydrogenation was carried out with the catalyst formed by decarbonylation of γ-Al_2O_3-supported $[Ir_6(CO)_{15}]^{2-}$ as a result of treatment in He at 300 °C for 2 h. The iridium clusters in the unused catalyst are represented as Ir_6 on the basis of the EXAFS results stated above. The catalytic activity was measured in a once-through flow reactor under the following conditions: $P_{H_2} = 710$ Torr, $P_{toluene} = 50$ Torr, temperature = 60, 80, or 100 °C. The catalyst achieved a stable steady state in operation after an induction period of typically an hour and remained stable for at least 20 h on stream (Figure 8). The reported rate data correspond to steady-state operation following the induction period. The rates were determined from differential conversions[10] less than about 0.2%, and they are represented as turnover frequencies in units

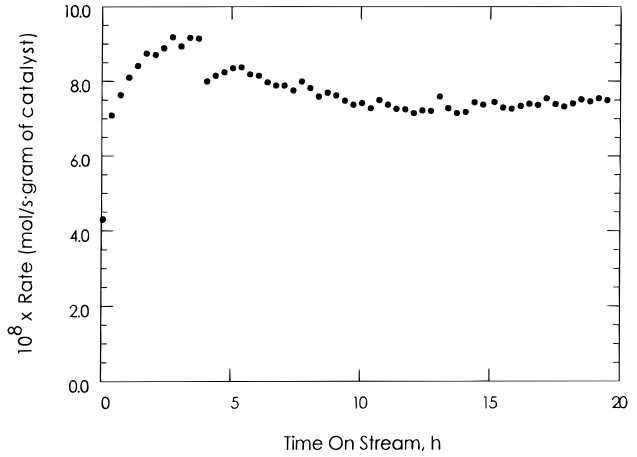

Figure 8. Toluene hydrogenation catalyzed by γ-Al_2O_3-supported Ir_6 clusters in a flow reactor: evidence of stability of the catalyst. Reaction conditions: $P_{toluene} = 50$ Torr, $P_{H_2} = 710$ Torr, temperature = 60 °C.

Table 3. Kinetics of Toluene Hydrogenation Catalyzed by Iridium Catalysts at $P_{toluene} = 50$ Torr and $P_{H_2} = 710$ Torr

reaction temp (°C)	$10^3 \times$ catalytic activity (molecules of toluene/(Ir atom·s))	
	Ir_6/γ-Al_2O_3	$Ir_{aggregates}/\gamma$-Al_2O_3[a]
60	1.7	9.7
80	3.8	17.7
100	7.3	35.3

[a] The activity is stated per total Ir atom in the catalyst.

of [molecules of toluene converted (Ir atom·s)$^{-1}$], as summarized in Table 3. The apparent activation energy determined from the temperature dependence of the turnover frequency was found to be 9.0 ± 0.7 kcal/mol, which is approximately the same as that reported for toluene hydrogenation catalyzed by supported Pt and Pd catalysts consisting of metallic particles on metal oxide supports.[25,26]

B. Iridium Aggregates Supported on γ-Al_2O_3. Toluene hydrogenation experiments were done in the same way with the catalyst consisting of aggregates of iridium on the γ-Al_2O_3 support. The iridium aggregates (crystallites) were formed by treatment of γ-Al_2O_3-supported $[Ir_4(CO)_{12}]$ in He at 400 °C for 1.5 h, followed by treatment in H_2 at 400 °C for 1 h and purging in He at 400 °C for 0.5 h. The rates of toluene hydrogenation observed for this catalyst (Table 3) are reported per total Ir atom; thus the rates characterizing the iridium aggregates are not turnover frequencies because not all the iridium atoms were surface atoms, as shown by EXAFS results stated below. Thus the comparison of activities of the two catalysts per total Ir atom (Table 3) understates the intrinsic difference in their activities.

Characterization of Used Iridium Catalyst by EXAFS Spectroscopy. A. Ir_6/γ-Al_2O_3. A sample of Ir_6/γ-Al_2O_3 catalyst that had been used in the flow reactor for 4 h on stream at 60 °C with a H_2 partial pressure of 710 Torr and a toluene partial pressure of 50 Torr was characterized by EXAFS

(25) Lin, S. D.; Vannice, M. A. *J. Catal.* **1993**, *143*, 554.
(26) Rahaman, M. V.; Vannice, M. A. *J. Catal.* **1991**, *127*, 251.

Table 4. EXAFS Results Characterizing Ir_6/γ-Al_2O_3 after Use as a Catalyst for Toluene Hydrogenation under the Following Conditions: $P_{toluene} = 50$ Torr, $P_{H_2} = 710$ Torr, Temperature = 60 °C[a,b]

shell	coordination no., N	distance, r, Å	$10^3 \times$ Debye−Waller factor, $\Delta\sigma^2$, Å^2	inner potential corr, ΔE_0, eV	EXAFS ref
Ir−Ir	4.05 ± 0.04	2.701 ± 0.001	4.59 ± 0.08	−2.22 ± 0.09	Pt−Pt
Ir−$O_{support}$					
Ir−O_s	1.04 ± 0.01	2.221 ± 0.001	7.42 ± 0.24	−18.70 ± 0.11	Pt−O
Ir−O_l	0.82 ± 0.01	2.723 ± 0.001	−5.92 ± 0.13	−13.20 ± 0.12	Pt−O
Ir−Al	0.37 ± 0.01	1.518 ± 0.001	8.12 ± 0.22	17.03 ± 0.33	Ir−Al

[a] The catalyst had been used for 4 h in the flow reactor. [b] The error bounds stated here were obtained from the statistical analysis of the data; they indicate the precisions, not accuracies.

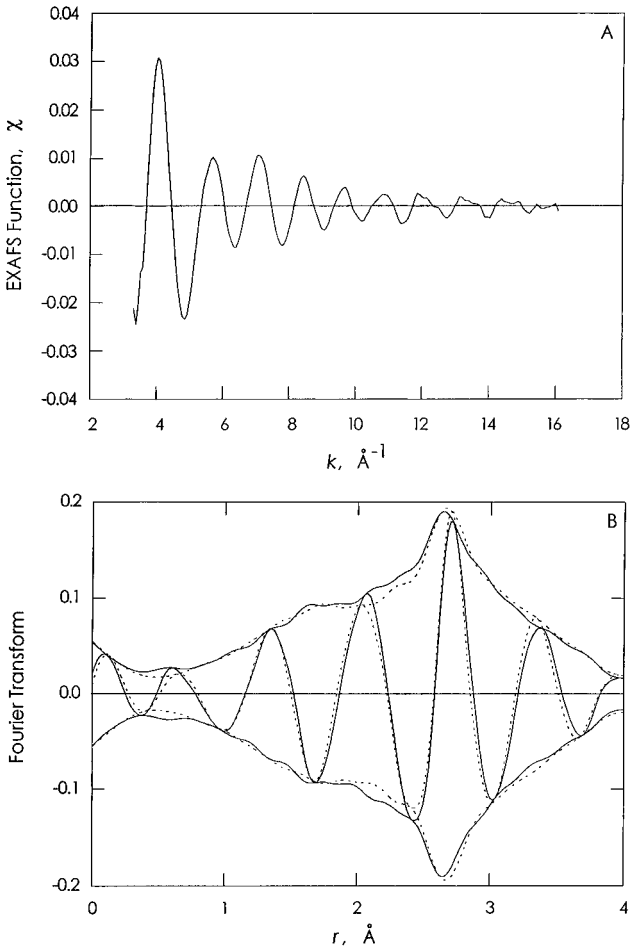

Figure 9. Results of EXAFS analysis characterizing the used Ir_6/γ-Al_2O_3 catalyst for toluene hydrogenation after being on stream for 4 h at 60 °C under $P_{toluene} = 50$ Torr and $P_{H_2} = 710$ Torr: (A) raw EXAFS data; (B) imaginary part and magnitude of Fourier transform (unweighted; $\Delta k = 3.69-14.99$ Å^{-1}; Pt−Pt phase and amplitude corrected) of raw EXAFS function of fresh Ir_6/γ-Al_2O_3 catalyst (solid line) and used Ir_6/γ-Al_2O_3 catalyst (dashed line).

spectroscopy. The normalized EXAFS function was obtained from the average of the X-ray absorption spectra from six scans, with the standard deviations in the EXAFS function being less than 0.0005 over the whole range of k space; the raw EXAFS data show oscillations up to 16 Å^{-1} (Figure 9A). The data analysis was performed as for the fresh catalyst; details are given in the section entitled EXAFS Data Analysis.

The data analysis indicated the following contributions: Ir−Ir, Ir−O_s, Ir−O_l, and Ir−Al. The structural parameters and the standard deviations are summarized in Table 4. The number of parameters used to fit the data is 16; the statistically justified number, calculated from the Nyquist theorem ($\Delta k = 11.3$ Å^{-1}, $\Delta r = 5$ Å), is approximately 37.

The Fourier transforms of the raw EXAFS data characterizing the fresh and used Ir_6 catalysts are shown in Figure 9B; they are almost indistinguishable from each other, indicating that there was almost no change in the catalyst structure during operation. Consistent with this conclusion, the Ir−Ir first-shell coordination number of the used catalyst was found to be 4.05 ± 0.04, which is indistinguishable from the value for the fresh Ir_6/γ-Al_2O_3 catalyst (Table 2). Thus we conclude that the octahedral metal frame remained intact during catalysis; this result is consistent with the lack of catalyst deactivation in the steady-state flow reactor experiments.

B. Iridium Aggregates Supported on γ-Al_2O_3. A sample consisting of iridium aggregates supported on γ-Al_2O_3 that had been used in the flow reactor for 4 h on stream at 60 °C with a H_2 partial pressure of 710 Torr and a toluene partial pressure of 50 Torr was also characterized by EXAFS spectroscopy. The EXAFS data were analyzed by the method stated for the Ir_6/γ-Al_2O_3 catalyst, except that higher-shell Ir−Ir contributions were significant and accounted for. The structural parameters with the standard deviations are summarized in Table 5. The data indicate an average first-shell Ir−Ir coordination number of 7.89 ± 0.07. Thus, this catalyst consisted of small (and no doubt nonuniform) particles of iridium dispersed on the γ-Al_2O_3 support. The first-shell Ir−Ir coordination number corresponds to aggregates with a dispersion of about 70%, consisting of about 50 atoms per aggregate, on average.[27] Thus, not all of the iridium atoms were surface atoms, and the representation of the rate of toluene hydrogenation per total Ir atom is an under approximation of the turnover frequency.

Discussion

Chemistry of Formation of $[Ir_6(CO)_{15}]^{2-}$ on γ-Al_2O_3. A. Evidence of Formation of $[Ir_6(CO)_{15}]^{2-}$. The results of the infrared spectroscopy, EXAFS spectroscopy, and mass spectrometry experiments show that $[Ir_6(CO)_{15}]^{2-}$ formed from [Ir(CO)$_2$(acac)] on the γ-Al_2O_3 surface. The EXAFS data indicate the octahedral metal frame as well as two terminal carbonyl ligands per Ir atom, as discussed below; both of these results are consistent with the crystallographically determined structure of $[Ir_6(CO)_{15}]^{2-}$.[28]

The infrared spectrum of the species extracted from the γ-Al_2O_3 surface with [PPN][Cl] in THF matches that of the PPN salt of $[Ir_6(CO)_{15}]^{2-}$,[14] except for minor peaks that are well identified with other iridium carbonyls. The mass spectrometry data are also consistent with the identification of $[Ir_6(CO)_{15}]^{2-}$ as the cluster extracted from the surface. Furthermore, the infrared spectrum of the adsorbed species identified as $[Ir_6(CO)_{15}]^{2-}$ agrees well with that of the MgO-supported iridium carbonyl identified as this cluster anion.[13]

The result that $[Ir_6(CO)_{15}]^{2-}$ was formed on the γ-Al_2O_3 surface in high yield confirms that surface-mediated synthesis[29]

(27) Kip, B. J.; Duivenvoorden, F. B. M.; Koningsberger, D. C.; Prins, R. *J. Catal.* **1987,** *105*, 26.
(28) Demartin, F.; Manassero, M.; Sansoni, M.; Garlaschelli, L.; Martinengo, S.; Canziani, F. *J. Chem. Soc., Chem. Commun.* **1980**, 903.
(29) Gates, B. C. *J. Mol. Catal.* **1994**, *86*, 95.

Table 5. EXAFS Results Characterizing the Ir_{agg}/γ-Al_2O_3 Catalyst That Had Been Used for Toluene Hydrogenation under the Following Conditions: $P_{toluene} = 50$ Torr, $P_{H_2} = 710$ Torr, Temperature = 60 °C[a,b]

shell	coordination no., N	distance, r, Å	$10^3 \times$ Debye−Waller factor, $\Delta\sigma^2$, Å^2	inner potential corr, ΔE_0, eV	EXAFS ref
Ir−Ir (1)[c]	7.89 ± 0.07	2.693 ± 0.000	4.26 ± 0.05	−1.91 ± 0.08	Pt−Pt
Ir−Ir (2)[d]	6.68 ± 0.15	3.806 ± 0.003	9.10 ± 0.30	−1.77 ± 0.17	Pt−Pt
Ir−Ir (3)[e]	5.66 ± 0.19	4.673 ± 0.003	4.87 ± 0.42	0.38 ± 0.23	Pt−Pt
$Ir-O_{support}$					
$Ir-O_s$	0.96 ± 0.01	2.116 ± 0.002	5.05 ± 0.33	0.34 ± 0.15	Pt−O
$Ir-O_l$	0.49 ± 0.01	2.722 ± 0.002	−8.37 ± 0.14	−10.28 ± 0.32	Pt−O
Ir−Al	0.56 ± 0.04	1.521 ± 0.008	10.88 ± 0.93	20.31 ± 1.57	Ir−Al

[a] The catalyst had been used for 4 h in the flow reactor. [b] The error bounds stated here were obtained from the statistical analysis of the data; they indicate the precisions, not accuracies. [c] Ir−Ir(1) represents the first-shell Ir−Ir contribution. [d] Ir−Ir(2) represents the second-shell Ir−Ir contribution. [e] Ir−Ir(3) represents the third-shell Ir−Ir contribution.

is an efficient method for preparation of this cluster; this work extends the synthesis of this cluster to γ-Al_2O_3.

The ν_{CO} spectrum of the surface-bound iridium carbonyl cluster is shifted and broadened with respect to the solution spectrum of $[Ir_6(CO)_{15}]^{2-}$. The peak broadening is typical of supported metal carbonyls, being explained by the nonuniformity of the γ-Al_2O_3 surface. The shift of both the terminal and bridging ν_{CO} bands to higher frequencies is indicative of electron withdrawal from the metal framework, possibly by Al^{3+} sites on the γ-Al_2O_3 surface with which the clusters interact. Consequently, the backbonding due to the interaction between the d orbital of the iridium atom and the antibonding orbital of the CO ligand is decreased and the C−O bond is strengthened, resulting in the increase of the carbonyl stretching frequency.

The postulated Ir−Al interaction is consistent with the results of the EXAFS data analysis for $[Ir_6(CO)_{15}]^{2-}$ supported on γ-Al_2O_3, as shown in Table 1, but we emphasize that this EXAFS contribution is small and not determined with a high degree of confidence. Perhaps the $[Ir_6(CO)_{15}]^{2-}$ on γ-Al_2O_3 is distorted, allowing Ir−Al interactions; alternatively, the Ir−Al contribution could be an indication of mononuclear species such as iridium subcarbonyls on the surface. The data are not sufficient to distinguish among the possible interpretations.

The observed shifts are different from some reported for metal carbonyl clusters on metal oxide supports. Often, the interaction of a metal carbonyl with a metal oxide support leads to shifts to higher frequency of terminal CO bands accompanied by shifts to lower frequency of bridging CO bands.[30,31] Such shifts have been interpreted as a consequence of electron withdrawal from the cluster by surface cations (leading to shifts to higher frequencies of the terminal CO bands) and simultaneous interaction of the oxygen atoms of bridging CO ligands with neighboring surface cations (leading to a shift to lower frequency of the bridging CO bands). This explanation is consistent with that of Shriver et al.[32,33] for the shifts of ν_{CO} bands resulting from adduct formation between $[(C_5H_5)Fe(CO)_2]_2$ and Lewis acids such as $Al(C_2H_5)_3$. Since, in the present work, we did not observe a shift to lower frequency of the bridging CO band, we suggest that the bridging CO ligands did not interact directly with surface Al^{3+} ions; this suggestion is consistent with the expectation that the Al^{3+} sites on the γ-Al_2O_3 surface were largely covered with OH groups in our samples,[23] which had not been treated at the high temperatures that give high degrees of surface dehydroxylation.

Influence of Surface Water Content. Water affected the surface chemistry. Infrared spectra of the iridium carbonyl species formed from $[Ir(CO)_2(acac)]$ on γ-Al_2O_3 (Figure 4) indicate that $[Ir_6(CO)_{15}]^{2-}$ formed on the γ-Al_2O_3 that had not been calcined (and thus was hydroxylated). This conclusion supports the hypothesis that traces of water or OH groups on the surface of γ-Al_2O_3 could have facilitated the reductive carbonylation process to form $[Ir_6(CO)_{15}]^{2-}$.[34] Angoletta et al.[16] reported that the reaction of $[Ir_4(CO)_{12}]$ with sodium in wet THF gives $[Ir_6(CO)_{15}]^{2-}$, which is not formed in dry THF. The authors proposed that nucleophilic attack on the CO ligands by OH^- groups facilitates the reduction of iridium and the oxidation of CO to CO_2. Chini and Martinengo[35] observed a large effect of water on the synthesis of $[Rh_6(CO)_{16}]$ and of $[Rh_4(CO)_{12}]$ from $[Rh(CO)_2Cl]_2$ and CO in organic solvents; the surface synthesis of $[Rh_6(CO)_{16}]$ from $[Rh(I)(CO)_2]$ species on η-Al_2O_3[36] is analogous to this solution synthesis, with water playing a key role. The formation of $[Rh_6(CO)_{16}]$ on the η-Al_2O_3 surface was found to be facile in the presence of both CO and excess water; removal of the excess water by evacuation resulted in the destruction of the cluster frame and the appearance of the oxidized species, $[Rh(I)(CO)_2]$.

In contrast, tetrairidium carbonyls (in a mixture with mononuclear iridium carbonyls) formed from $[Ir(CO)_2(acac)]$ on γ-Al_2O_3 that had been calcined at 300 °C and thereby was about 50% dehydroxylated.[23] The results thus indicate that the partially dehydroxylated surface favors the formation of tetranuclear rather than hexanuclear clusters, although the conversion to the tetranuclear cluster was not complete. The infrared spectrum of this mixture (Figure 4C) is nearly the same as that of the sample formed by recarbonylation of the decarbonylated $[Ir_6(CO)_{15}]^{2-}$ on γ-Al_2O_3 (Figure 6E). This agreement suggests that the degree of surface dehydroxylation of the latter sample resulting from the thermal treatment in He at 300 °C was about the same as that of the partially dehydroxylated sample in which the mixture including tetranuclear iridium carbonyl formed initially from $[Ir(CO)_2(acac)]$.

In summary, the results demonstrate that water (or surface hydroxyl groups) was important in the synthesis of metal carbonyl clusters on metal oxide surfaces, consistent with related solution chemistry.

Reductive Carbonylation and Oxidative Fragmentation Cycle. Treatment of $[Ir(CO)_2(acac)]$ adsorbed on γ-Al_2O_3 under CO at 100 °C led to the formation of $[Ir_6(CO)_{15}]^{2-}$. When the γ-Al_2O_3-supported $[Ir_6(CO)_{15}]^{2-}$ was exposed to air, a reaction occurred to yield surface species which are identified as a

(30) Kawi, S.; Chang, J.-R.; Gates, B. C. *J. Am. Chem. Soc.* **1993**, *115*, 4830.

(31) Rao, L.-F.; Fukuoka, A.; Kosugi, N.; Kuroda, H.; Ichikawa, M. *J. Phys. Chem.* **1990,** *94*, 5317.

(32) Shriver, D. F. *J. Organomet. Chem.* **1975**, *94*, 259.

(33) Horwitz, C. P.; Shriver, D. F. *Adv. Organomet. Chem.* **1984**, *23*, 219.

(34) In the present work, the content of surface hydroxyl groups could be estimated approximately on the basis of the intensity of the ν_{OH} band (3000−3750 cm^{-1}) in the infrared spectra of γ-Al_2O_3 supports calcined at different temperatures. The ν_{OH} bands decreased in intensity and shifted to higher frequencies as the support calcination temperature increased.

(35) Chini, P.; Martinengo, S. *Inorg. Chim. Acta* **1969**, *3*, 315.

(36) Smith, A. K.; Hugues, F.; Theolier, A.; Basset, J. M.; Ugo, R.; Zanderighi, G. M.; Bilhou, J. L.; Bilhou-Bougnol, V.; Graydon, W. F. *Inorg. Chem.* **1979**, *18*, 3104.

mixture of [Ir(I)$(CO)_2$] and [$Ir_4(CO)_{12}$] on the basis of a comparison of the infrared spectrum with the spectra of [Ir$(CO)_2$(acac)] and [$Ir_4(CO)_{12}$] adsorbed on γ-Al_2O_3.

The oxidized iridium carbonyls on γ-Al_2O_3 were reductively carbonylated by treatment in CO at 100 °C to give back $[Ir_6(CO)_{15}]^{2-}$. Kawi et al.[30] similarly reported an oxidative fragmentation/reductive carbonylation cycle involving [$Ir_6(CO)_{16}$] and [Ir(I)$(CO)_2$] in the pores of NaY zeolite and suggested that the zeolite cages played a role in confining the supported metal carbonyls and hindering their migration out of the pores. Smith et al.[36] reported a cycle involving [$Rh_6(CO)_{16}$] and [Rh(I)$(CO)_2$] on η-Al_2O_3 and presumed that the oxidized species were weakly bound to each other to facilitate the reversible transformation at room temperature. Adopting this reasoning, we suggest that there was perhaps little change in the location of the iridium atoms on the γ-Al_2O_3 surface during the reversible cycle, since the recarbonylation reaction was facile. Thus the fragmented clusters were perhaps clusters in their own right; a similar suggestion was made on the basis of transmission electron microscopy for triosmium clusters formed from [$Os_3(CO)_{12}$] on γ-Al_2O_3.[37]

Parallels between Solution Chemistry and Surface Chemistry of Iridium Carbonyl Clusters. There is a rich solution chemistry of iridium carbonyl clusters. Reductive carbonylation of $IrCl_3 \cdot 3H_2O$ in weakly acidic solutions under CO leads to $[Ir(CO)_2Cl_2]^-$, which was subsequently transformed into [$Ir_4(CO)_{12}$] when the solution was neutralized.[22] In basic solutions, the reaction of [$Ir_4(CO)_{12}$] under CO yields anionic iridium carbonyl clusters, $[HIr_4(CO)_{11}]^-$ and then $[Ir_6(CO)_{15}]^{2-}$ as the solution basicity is increased.[16] The latter is converted to [$Ir_6(CO)_{16}$] in acidic media.[16,38,39]

One can make a good beginning toward understanding of the chemistry of iridium carbonyls on metal oxide surfaces by comparing the functional groups of the surface with those of solvents. Syntheses of metal carbonyl clusters on some metal oxide surfaces are comparable to those in neutral or basic solutions; the metal oxide surface plays a role analogous to that of a basic solvent.[29] Evidently, both MgO[13,15] and γ-Al_2O_3 have sufficiently basic surfaces to provide efficient media for the synthesis of anionic iridium carbonyl clusters (and the degree of hydroxylation is important). Chemistry similar to that reported here also occurs in the cages of NaX zeolite.[40] In contrast, neutral iridium carbonyl clusters, [$Ir_4(CO)_{12}$] and [$Ir_6(CO)_{16}$], rather than anions, form as a result of similar reactions in the cages of NaY zeolite,[30,41] which is less basic than NaX zeolite, and on the nearly neutral SiO_2.[42]

The iridium carbonyl chemistry on the surface of γ-Al_2O_3 is, however, more complicated than what is stated in the preceding paragraph. The reaction of monovalent iridium dicarbonyl precursors on γ-Al_2O_3 in CO at room temperature yields the neutral iridium carbonyl cluster [$Ir_4(CO)_{12}$].[11] In this work, the same precursors in CO at 100 °C were converted into anionic hexairidium carbonyl clusters. Thus there are subtleties in the surface chemistry that are not yet well understood. The results support the suggestion that the γ-Al_2O_3 surface is intermediate in basicity between that of partially dehydroxylated MgO and that of NaY zeolite or even SiO_2. We emphasize, however, the reactivity of the γ-Al_2O_3 surface depends on the temperature as well as the degree of hydroxylation.

Confirmation by EXAFS Spectroscopy of the Structure of $[Ir_6(CO)_{15}]^{2-}$ on γ-Al_2O_3. The EXAFS results support the identification of $[Ir_6(CO)_{15}]^{2-}$ on γ-Al_2O_3. The backscatterers in the immediate vicinity of the iridium absorber atoms in the γ-Al_2O_3-supported iridium carbonyls include Ir and low-atomic-weight backscatterers identified by the multiple scattering effects as C and O*. The structural parameters agree, within experimental error, with the crystallographic data for $[Ir_6(CO)_{15}]^{2-}$.[28] The crystal structure of $[Ir_6(CO)_{15}]^{2-}$ (in the $[NMe_3CH_2Ph]^+$ salt) is that of an essentially regular octahedron of iridium atoms connected to 12 terminal and three symmetrically edge-bridging CO ligands. All the iridium atoms are stereochemically equivalent, with each bonded to four iridium atoms at an average distance of 2.773 Å, to two terminal carbonyl ligands with an average Ir−C_t distance of 1.860 Å, and to one bridging CO ligand with an average Ir−C_b distance of 2.038 Å. The EXAFS data indicate an Ir−Ir first-shell coordination number of 4.07 with an average distance of 2.75 Å, an Ir−C_t coordination number of 2.13 with an average distance of 1.87 Å, and an Ir−C_b coordination number of 1.17 with an average distance of 2.19 Å (Table 1).

Thus all the EXAFS results except that characterizing the Ir−O* interaction agree approximately with the crystallographic data for $[Ir_6(CO)_{15}]^{2-}$; the coordination number for Ir−O* is 2.03 instead of the expected 3. The discrepancy can be understood on the basis of multiple scattering effects;[13,43,44] it is a result of the existence of two types of carbonyl oxygen contribution at nearly the same distance but experiencing different degrees of multiple scattering, leading to a low estimate of the Ir−O* coordination number; the same discrepancy has been reported by Maloney et al.[13] and Kawi et al.[30]

The lack of exact agreement between the other structure parameters for the supported $[Ir_6(CO)_{15}]^{2-}$ clusters determined by EXAFS spectroscopy and those determined crystallographically for the salt of $[Ir_6(CO)_{15}]^{2-}$ is attributed to (1) interactions between the γ-Al_2O_3 surface and the clusters (which affect the structure of the supported clusters), (2) the presence of small amounts of other iridium carbonyls on the surface (which affect the EXAFS data), and (3) the inexactness of the EXAFS analysis associated with the approximations in the theory.[45] We are not yet able to resolve the separate issues; we emphasize that the error bounds stated with the EXAFS parameters (Table 1) are measures only of the precision of the parameter estimates.

EXAFS Results Characterizing Decarbonylated Iridium Clusters Supported on γ-Al_2O_3. The γ-Al_2O_3-supported iridium clusters were formed by decarbonylation of $[Ir_6(CO)_{15}]^{2-}$ on γ-Al_2O_3; infrared spectra showed the complete disappearance of the ν_{CO} bands after thermal treatment in He at 300 °C for 2 h.

The raw EXAFS data characterizing these γ-Al_2O_3-supported iridium clusters show oscillations up to a value of k of 17 $Å^{-1}$; the data quality is very high. The data analysis showed a first-shell Ir−Ir coordination number of 4.05 ± 0.07. Thus the results are consistent with the identification of the clusters as octahedral

(37) Schwank, J.; Allard, L. F.; Deeba, M.; Gates, B. C. *J. Catal.* **1983**, *84*, 27.
(38) Garlaschelli, L.; Martinengo, S.; Bellon, P. L.; Demartin, F.; Manassero, M.; Chiang, M. Y.; Wei, C.-Y.; Bau, R. *J. Am. Chem. Soc.* **1984**, *106*, 6664.
(39) Stevens, R. E.; Liu, P. C. C.; Gladfelter, W. L. *J. Organomet. Chem.* **1985**, *287*, 133.
(40) Kawi, S.; Chang, J.-R.; Gates, B. C. *J. Catal.* **1993**, *142*, 585.
(41) Kawi, S.; Gates, B. C. *Catal. Lett.* **1991**, *10*, 263.
(42) Roberto, D.; Cariati, E.; Psaro, R.; Ugo, R. *J. Organomet. Chem.* **1995**, *488*, 109.
(43) van Zon, F. B. M.; Kirlin, P. S.; Gates, B. C.; Koningsberger, D. C. *J. Phys. Chem.* **1989**, *93*, 2218.
(44) The contribution from the oxygens of the bridging carbonyl ligands could be minimal in the total EXAFS since the multiple-scattering effect is not significant when the Ir−C−O bond angle is less than approximately 140°. In crystalline $[Ir_6(CO)_{15}]^{2-}$, the Ir−C−O_t angle is 176°, whereas the Ir−C−O_b angle is 138°.[13]
(45) Stern, E. A. In *X-ray Absorption: Principles, Applications, Techniques of EXAFS, SEXAFS, and XANES;* Koningsberger, D. C., Prins, R., Eds.; Wiley: New York, 1988; p 3.

Ir_6 clusters. The data show that the metal frame of $[Ir_6(CO)_{15}]^{2-}$ supported on γ-Al_2O_3 was retained after cluster decarbonylation. We conclude that the supported Ir_6 clusters are nearly uniform and nearly molecular in character, being among the best defined supported metals.

The lack of peaks in the Fourier transform corresponding to higher-shell Ir−Ir neighbors is consistent with the inference that there was no significant sintering of iridium to form larger clusters or crystallites on the γ-Al_2O_3 surface.

Decarbonylation of supported iridium carbonyl clusters with (near) retention of the metal frame has been reported to give Ir_4 on MgO,[24,46] on γ-Al_2O_3,[11] in NaY zeolite,[47] and in NaX zeolite.[48] These results demonstrate the preparation of nearly uniform, structurally well-defined metal clusters by decarbonylation of metal carbonyl precursors;[9] similarly, Ir_6 clusters were formed in NaY zeolite.[30] The work reported here extends the preparation method to Ir_6 clusters on an amorphous metal oxide support; earlier work involving decarbonylation of hexairidium carbonyl anions on MgO led to mixtures of clusters, including Ir_6.[46]

EXAFS Results Characterizing Used Ir_6/γ-Al_2O_3 and Used Ir_{agg}/γ-Al_2O_3 Catalysts. A sample of Ir_6/γ-Al_2O_3 used as a catalyst for toluene hydrogenation was characterized by EXAFS spectroscopy. The good agreement between the Fourier transform of the raw EXAFS data representing the fresh catalyst and that representing the used catalyst (Figure 9B) indicates that the structure of the clusters in the catalyst was maintained during the catalysis. Analysis of the EXAFS data for the used catalyst confirms the conclusion; the results showed an Ir−Ir coordination number of 4.05 ± 0.04, consistent with octahedral Ir_6 clusters.

Recently communicated results[10] indicate that Ir_4 and Ir_6 supported on MgO, Ir_4 on γ-Al_2O_3, and Ir_6 in NaY zeolite remained almost unchanged during toluene hydrogenation catalysis under conditions the same as those used in this work. The data presented here, being of higher quality, strengthen the conclusion and demonstrate the stability of the supported iridium clusters. Similarly, Kawi et al.[49] found that Ir_4 clusters on MgO remained intact during catalysis of propane hydrogenolysis at 200 °C. Thus this family of supported iridium clusters offers a unique opportunity to resolve the effects of cluster nuclearity and support structure on the catalytic properties of metal clusters.

The EXAFS data for the used catalyst consisting of iridium aggregates on γ-Al_2O_3 demonstrate the presence of particles characterized by first-, second-, and third-shell Ir−Ir contributions; thus these particles have much more of the character of bulk iridium than the Ir_6 clusters. The average first-shell Ir−Ir distance in these particles is 2.693 Å; the Ir−Ir distance in bulk iridium metal, determined by X-ray diffraction, is 2.714 Å.[50] Within the accuracy of the EXAFS determination, these two values are indistinguishable. For comparison, the Ir−Ir distance in Ir_6/γ-Al_2O_3 was found to be 2.704 Å for the unused catalyst and 2.701 Å for the used catalyst; within the experimental accuracy, these values are also indistinguishable from the value for bulk iridium.

Catalytic Properties of Ir_6 Clusters and Iridium Aggregates for Toluene Hydrogenation. The catalytic activity of Ir_6 on γ-Al_2O_3 is low relative to that of iridium aggregates (crystallites) on the same support (Table 3), which are more nearly metallic in character.[10] Similarly, the catalytic activities of Ir_4 and Ir_6 on MgO are low relative to that of iridium aggregates on MgO.[10] Therefore, although the extremely small iridium clusters catalyze at least two of the same reactions as metallic iridium,[10,51] their catalytic character is significantly different, with the catalytic activity of the aggregates being greater than that of the clusters, even though their Ir−Ir distances are the same within the experimental accuracy of the EXAFS measurements.

Thus the concept of structure insensitivity[5] in metal catalysis may be limited to virtually metallic surfaces and may not extend to the smallest metal clusters on supports. Boudart and Sajkowski[52] measured turnover frequencies for the structure-insensitive cyclohexene hydrogenation with a family of alumina-supported rhodium catalysts, finding that the turnover frequency remained essentially unchanged as the aggregate or cluster nuclearity of the fresh catalyst became as small as approximately 12 atoms, on average, as estimated by EXAFS spectroscopy. Combining our results and those of Boudart and Sajkowski (and assuming that there was no aggregation of the metal in their catalyst during catalysis) leads to the suggestion that the changes in turnover frequency occur predominantly as the cluster nuclearity becomes smaller than approximately 12.

It is perhaps surprising that such a large change in turnover frequency as shown in Table 3 would result from a change in aggregate or cluster nuclearity to 6 even though the Ir−Ir distance remained unchanged within the accuracy of the EXAFS measurements. We emphasize that the present results do not simply demonstrate the influence of cluster or aggregate size on the catalytic activity; the influence of the support on the metal oxidation state and catalytic properties is no doubt dependent on the cluster or aggregate size, and it may well be that the decrease in catalytic activity as the aggregates become smaller and approach the size of Ir_6 clusters is largely a consequence of the increasing effect of the γ-Al_2O_3 support as a ligand bonded to the iridium and making it less like bulk, metallic iridium. There are not yet sufficient data to resolve the effects of cluster size and support ("ligand") effects.

The γ-Al_2O_3-supported Ir_6 clusters are stable catalysts, as shown both by the lack of significant changes in their activities during steady-state operation in a flow reactor and by the EXAFS results indicating retention of the metal framework during catalysis. Thus the supported clusters appear to be robust enough to be applied as practical catalysts, at least under relatively mild conditions; furthermore, the reversible cycles of cluster formation and fragmentation even suggest opportunities for catalyst regeneration. The novel catalytic properties of the supported clusters raise the possibility that reactions may be found for which such clusters have catalytic properties (e.g., selectivity) better than those of conventional supported metals, but this suggestion remains to be evaluated.[10]

A comparison of the data presented here with those of Xu et al.[10] indicates that the γ-Al_2O_3-supported Ir_6 clusters are an order of magnitude more active than MgO-supported Ir_6 clusters. This comparison is a first step toward elucidation of support effects in catalysis by metal clusters, but more data are needed to elucidate the influence of catalyst pretreatment and the density of surface OH groups.

EXAFS Spectroscopy Characterizing Metal−Support Interaction. The EXAFS data provide information about the interactions between the γ-Al_2O_3 support and the iridium clusters. The data indicate Ir−O contributions at two different

(46) van Zon, F. B. M.; Maloney, S. D.; Gates, B. C.; Koningsberger, D. C. *J. Am. Chem. Soc.* **1993,** *115,* 10317.
(47) Kawi, S.; Chang, J.-R.; Gates, B. C. *J. Phys. Chem.* **1993**, *97*, 10599.
(48) Kawi, S.; Gates, B. C. *J. Phys. Chem.* **1995**, *99*, 8824.
(49) Kawi, S.; Chang, J.-R.; Gates, B. C. *J. Phys. Chem.* **1994**, *98*, 12978.
(50) Weast, R. C.; Astle, M. J., Eds. *Handbook of Chemistry and Physics*; CRC Press: Boca Raton, FL, 1980; F-219.
(51) Xu, Z.; Gates, B. C. *J. Catal.* **1995**, *154*, 335.
(52) Boudart, M.; Sajkowski, D. J. *Faraday Discuss. Chem. Soc.* **1991**, *92*, 57.

distances, 2.2 and 2.7 Å. Metal−oxygen contributions at approximately these same distances have been observed frequently for metal oxide-supported noble metals.[53] The shorter distance is suggestive of metal−oxygen bonding, with the metal perhaps bearing a positive charge.[54] The longer distance is not fully explained.[55]

In the present work, the high quality of the EXAFS data allowed identification of a small contribution suggested to be Ir−Al, for both $[Ir_6(CO)_{15}]^{2-}$ and Ir_6 clusters supported on γ-Al_2O_3. van Zon et al.[46] suggested a similar Ir−Mg contribution for decarbonylated iridium clusters supported on MgO; Otten et al.[56] reported a Pt−Al interaction for platinum clusters supported in the zeolite mordenite. However, the contribution suggested here was small and not identified with confidence, and the issues concerning such contributions are not fully understood; the data are not sufficient to determine the structure of the metal−support interface.

Purnell et al.[57] postulated that clusters may reside preferentially at defect sites on a MgO support, and we speculate that the iridium clusters exist at defects on the γ-Al_2O_3 surface, consistent with the suggested Ir−Al contributions in the EXAFS. If the speculation about the placement of the clusters at surface defects were correct, it might explain why the total loading of iridium carbonyl precursors on the γ-Al_2O_3 surface could not be increased beyond a few weight percent without causing significant structural changes.[58]

Experimental Section

Materials. $[Ir(CO)_2(acac)]$ [dicarbonyl(acetylacetonato)iridium(I), 99%, Strem] and [PPN][Cl] (Aldrich) were used as received. γ-Al_2O_3 (Aluminum Oxide C, Degussa) was made into a paste by adding deionized water, followed by drying overnight at 120 °C. It was then ground and evacuated at 25 °C overnight. The resultant γ-Al_2O_3 support was stored in a drybox. *n*-Hexane (>99.9% purity, Aldrich) and toluene (99.7%, J. T. Baker) were degassed by sparging of N_2 (99.997%, Liquid Carbonic) before use. THF (anhydrous, 99.9%, Aldrich) was dried by refluxing over sodium benzophenone ketyl under N_2 and degassed. He (99.995%) was supplied by Liquid Carbonic and passed through beds of Cu_2O and molecular sieve 4A to remove traces of O_2 and moisture. H_2 with a purity of 99.99% was generated by a Balston hydrogen generator and passed through the same beds used for He. CO was purchased from Liquid Carbonic (CP grade, 99.5%) and passed through a bed of γ-Al_2O_3 particles to remove traces of iron carbonyl contaminants and through a bed of molecular sieve particles to remove moisture.

Sample Preparation. Preparation and handling of the air-sensitive materials were carried out on a Schlenk vacuum line and in a Braun (MB-150M) glovebox filled with N_2 that was recirculated through traps to remove O_2 and water. Typical O_2 and water concentrations were <2 and 0.4 ppm, respectively.

Calcination. Partially dehydroxylated γ-Al_2O_3 was prepared as the γ-Al_2O_3 powder was heated in flowing O_2 to 100, 300, or 400 °C and then held at the final temperature for 2 h. The γ-Al_2O_3 was evacuated at the final temperature overnight, cooled under vacuum to room temperature, and unloaded in the glovebox.

Adsorption of $[Ir(CO)_2(acac)]$ on γ-Al_2O_3. The mononuclear iridium carbonyls supported on γ-Al_2O_3 were prepared by slurrying $[Ir(CO)_2(acac)]$ and γ-Al_2O_3 in degassed hexane (50 mL) in a Schlenk flask under a N_2 blanket. The mixture was stirred under N_2 for 12 h at room temperature and then dried by evacuation for 8 h at room temperature. The Ir content of the solid was calculated to be 1 wt % on the basis of the assumption that the uptake was complete during the preparation.

Infrared Spectroscopy. Transmission infrared spectra of the samples were collected with a Bruker IFS-66v spectrometer. Samples were pressed into thin self-supporting wafers and mounted in a sample holder in an infrared cell. The temperature-controlled cell, which was part of a flow system, was connected to a gas manifold allowing flow of He, H_2, and CO. The sample was typically heated to a set temperature and then scanned 64 times; the data were averaged. The spectra of the sample were ratioed to the spectrum of air.

Flow Reactor for Carbonylation. Carbonylation of mononuclear iridium species supported on γ-Al_2O_3 was carried out in a tubular flow reactor. Typically, 1 g of sample consisting of iridium carbonyl supported on γ-Al_2O_3 powder was loaded into the reactor and treated in flowing CO at 100 °C for 10 h. The powder was then unloaded in the drybox and characterized by infrared spectroscopy and EXAFS spectroscopy.

Extraction of Metal Carbonyl Clusters from γ-Al_2O_3. Surface-bound iridium carbonyls were extracted from the surface of γ-Al_2O_3 as the supported metal carbonyls were brought in contact with a solution of [PPN][Cl] in freshly distilled THF under N_2. The liquid was transferred by syringe into a solution infrared cell and quickly scanned. The spectra were ratioed to the spectrum of THF.

Mass Spectrometry. Fast atom bombardment mass spectrometry was performed with a VG-Analytical ZAB-2F mass spectrometer. The solution of iridium carbonyl clusters extracted by [PPN][Cl] in freshly distilled THF was placed on a stainless steel probe tip and vaporized prior to bombardment of the sample. The resultant ionic species were scanned between $m/z = 600$ and 2200 in the negative ion mode.

X-ray Absorption Spectroscopy. The experiments were performed on beamline X-11A of the National Synchrotron Light Source (NSLS) at Brookhaven National Laboratory, Upton, Long Island, NY, and on beamline 2-3 of the Stanford Synchrotron Radiation Laboratory (SSRL) at the Stanford Linear Accelerator Center, Stanford, CA. The storage ring operated with an electron energy of 2.5 GeV at NSLS and 3 GeV at SSRL; the beam current was 140−240 mA at NSLS and 70−100 mA at SSRL.

Wafers for the transmission EXAFS experiments were prepared in gloveboxes at the synchrotrons. The wafers were prepared as follows: Each powder sample was placed in a holder in the glovebox. The holder was placed in a pressing die, and the sample was pressed into a self-supporting wafer. After pressing, the sample in the holder was loaded into an EXAFS cell and sealed.

EXAFS data were recorded with the sample under vacuum and at approximately liquid nitrogen temperature. Higher harmonics in the X-ray beam were minimized by detuning the Si(111) double-crystal monochromator at NSLS by 15−20% or the Si(220) double-crystal monochromator at SSRL by 15−20% at the Ir L_{III} edge (11215 eV).

Precautions were taken to allow transport of the samples from the University of California at Davis to the synchrotrons without air contamination. Each sample was placed inside double layers of glass vials, each individually sealed with a vial cap and parafilm.

Toluene Hydrogenation Catalyzed by Supported Iridium. Toluene hydrogenation catalyzed by γ-Al_2O_3-supported iridium clusters or aggregates was carried out in a tubular flow reactor. The catalysts were pretreated *in situ* prior to the kinetics measurements. Typically, 40 mg of sample consisting of iridium carbonyl clusters supported on γ-Al_2O_3 powder was loaded into the reactor to give a thin catalyst bed. The precursors were either decarbonylated in He at 300 °C for 2 h to form supported iridium clusters or they were treated in flowing He at 400 °C for 1.5 h, followed by treatment in flowing H_2 at 400 °C for 1.0 h and then purging with He for 0.5 h at the same temperature to form iridium aggregates on γ-Al_2O_3. Toluene was degassed by purging with N_2 for 2 h before being charged to an Isco liquid metering pump (Model-260D). A reaction mixture consisting of H_2 and vaporized toluene at atmospheric pressure passed through the reactor at a total

(53) Koningsberger, D. C.; Gates, B. C. *Catal. Lett.* **1992**, *14*, 271.
(54) Chang, J.-R.; Gron, L. U.; Honji, A.; Sanchez, K. M.; Gates, B. C. *J. Phys. Chem.* **1991**, *95*, 9945.
(55) Vaarkamp, M.; Modica, F. S.; Miller, J. T.; Koningsberger, D. C. *J. Catal.* **1993**, *144*, 611.
(56) Otten, M. K.; Reifsnyder, S. N.; Lamb, H. H. *Physica B* **1995**, *209*, 651.
(57) Purnell, S. K.; Xu, X.; Goodman, D. W.; Gates, B. C. *J. Phys. Chem.* **1994**, *98*, 4076.
(58) The maximum loading of Ir on the uncalcined γ-Al_2O_3 obtained by the preparation method used in this work was found to be about 2 wt %; for comparison, if all the surface OH^- or O^{2-} sites could interact with the $[Ir(CO)_2(acac)]$ precursor, the loading would be expected to be about 20 wt % Ir.

Table 6. Structural Parameters Characterizing Reference Compounds and the Fourier Transform Range Used for Preparation of the Reference Files

	crystallographic data				Fourier transform[a]		
ref compd	shell	*N*	*r*, Å	ref	Δk, Å^{-1}	Δr, Å	*n*
Pt foil	Pt−Pt	12	2.77	64	1.9−19.8	1.9−3.0	3
$Na_2Pt(OH)_6$	Pt−O	6	2.05	65	1.4−17.7	0.5−2.0	3
$[Ir_4(CO)_{12}]$	Ir−C	3	1.87	66	2.8−16.5	1.1−2.0	3
	Ir−O*	3	3.01	66	2.8−16.5	2.0−3.3	3
IrAl alloy	Ir−Al[b]	8	2.58	46	2.7−12.0[c]	0.98−2.98	3

[a] Notation: Δk, limits of forward Fourier transform; Δr, limits of shell isolation; *n*, power of *k* used for Fourier transformation. [b] After subtraction of Ir−Ir contribution: $N = 6$, $r = 2.98$ Å, $\Delta\sigma^2 = -0.001$ Å^2, $\Delta E_0 = -3.3$ eV.[46] [c] A theoretical Ir−Al EXAFS function was calculated with the FEFF program[61] and adjusted to agree with the limited Ir−Al reference data obtained as described here for use of a larger interval in *k* space for fitting the iridium data.[46]

flow rate of 43 mL/min (NTP); the reactor was mounted in an electrically heated and temperature-controlled Lindberg furnace. The effluent gas mixture was analyzed with a Hewlett-Packard gas chromatograph (HP-5890 Series II) equipped with a DB-624 capillary column (J&W Scientific) and a flame ionization detector.

EXAFS Data Analysis

EXAFS Reference Data. The EXAFS data were analyzed with experimentally determined reference files obtained from EXAFS data for materials of known structure. The Ir−Ir and Ir−$O_{support}$ interactions were analyzed with phase shifts and backscattering amplitudes obtained from EXAFS data for Pt foil and $Na_2Pt(OH)_6$, respectively. The transferability of the phase shifts and backscattering amplitudes obtained from EXAFS data for platinum and iridium has been justified experimentally.[59] The Ir−C and Ir−O* interactions were analyzed with phase shifts and backscattering amplitudes obtained from EXAFS data for crystalline $[Ir_4(CO)_{12}]$ (which has only terminal CO ligands) mixed with SiO_2. $[Ir_4(CO)_{12}]$ was chosen because the multiple scattering effect in the Ir−O* shell is significant as a consequence of the linearity of the Ir−C−O moiety, and it was necessary to fit metal−carbonyl oxygen contributions with a reference that exhibits multiple scattering.[60] The Ir−Al interaction was analyzed with phase shifts and backscattering amplitudes obtained from a theoretical Ir−Al EXAFS function calculated with the FEFF program[61] and adjusted to agree with the Ir−Al reference data obtained from IrAl alloy.[46] The details of the preparation of the reference files are described elsewhere,[46,62,63] and the parameters used to extract these files from the EXAFS data are summarized in Table 6.

Analysis of EXAFS Data for $[Ir_6(CO)_{15}]^{2-}$ Supported on γ-Al_2O_3. The normalized EXAFS function characterizing $[Ir_6(CO)_{15}]^{2-}$ supported on γ-Al_2O_3 was obtained for each of six X-ray absorption spectra after a cubic spline background subtraction, followed by division by the height of the absorption edge. The raw EXAFS data shown in Figure 3A are an average of the results for the six scans. Because the infrared data indicate that carbonyl ligands were present in the sample, and because the metal atoms are expected to interact with the oxygen of the support, the data were first analyzed for Ir−Ir, Ir−C, Ir−O*, and Ir−$O_{support}$ interactions. The EXAFS analysis was done with experimentally determined reference files described in the section above entitled EXAFS Reference Data. The unweighted raw EXAFS data were fitted in *k* space over the range $3.50 < k < 16.45$ Å^{-1}; the data were also fitted in *r* space over the range $0 < r < 5$ Å, where *r* is the distance from the absorber Ir atom.

The analysis of the EXAFS data was performed with the Koningsberger difference file technique[63,67] and the XDAP data analysis software.[19] As a first step in the iterative analysis, the Ir−Ir contribution, the largest in the EXAFS spectrum, and the Ir−O* contribution were estimated from the reference data; since the Ir−O* contribution was found to be strongly coupled with the Ir−Ir contribution, these two contributions had to be analyzed simultaneously. Because the Ir−Ir contribution and the multiple scattering associated with the Ir−C−O* group are significant in the high-*k* range ($7.50 < k < 16.45$ Å^{-1}), with Ir−$O_{support}$ and Ir−C contributions being insignificant in this range, the structural parameters were estimated initially by fitting only the data in this range. Further analysis, following subtraction of the calculated Ir−Ir and Ir−O* contributions from the raw data, led to characterization of the Ir−C_t, Ir−C_b (where the subscripts t and b refer to terminal and bridging, respectively), and Ir−$O_{support}$ contributions. The initial guesses for parameter estimation were obtained by adjusting the coordination parameters to give the best fit of the residual spectrum both in *r* space and in *k* space. The fit of the raw data with the sum of the five contributions was still not satisfactory, and it was shown in the Fourier transform of the EXAFS function that an additional contribution involving an unknown backscatterer at a distance of about 1.5 Å from the Ir absorber atom had to be accounted for. The sixth contribution involved a low-atomic-number backscatterer, which could be the Al of the support; the contribution is thus referred to as Ir−Al, although it is so small that it could not be identified with confidence.

The structural parameters characterizing the Ir−C_t, Ir−C_b, Ir−$O_{support}$, and Ir−Al contributions were determined by fitting the residual spectrum. The calculated Ir−C, Ir−$O_{support}$, and Ir−Al contributions were subtracted from the raw data, and better estimates of the parameters representing the Ir−Ir and Ir−O* contributions were then estimated by fitting the residual spectrum. The iteration was continued until good overall agreement was obtained.

Analysis of EXAFS Data for Ir_6/γ-Al_2O_3. The normalized EXAFS function for the decarbonylated iridium clusters was obtained from the average of the X-ray absorption spectra from six scans. The data analysis was performed in *k* space over the range $3.68 < k < 16.26$ Å^{-1}, as well as in *r* space over the range $0 < r < 5$ Å, by using the unweighted raw EXAFS data. The Ir−Ir contribution was estimated by calculating an EXAFS function that agreed as closely as possible with the experimental

(59) Duivenvoorden, F. B. M.; Koningsberger, D. C.; Uh, Y. S.; Gates, B. C. *J. Am. Chem. Soc.* **1986,** *108,* 6254.
(60) Teo, B.-K. *J. Am. Chem. Soc.* **1981,** *103,* 3990.
(61) Lu, D.; Rehr, J. J. *J. Phys. (Paris) C8* **1986,** *47,* 67.
(62) van Zon, J. B. A. D. Ph.D. Dissertation, Eindhoven University of Technology, The Netherlands, 1988.
(63) van Zon, J. B. A. D.; Koningsberger, D. C.; van't Blik, H. F. J.; Sayers, D. E. *J. Chem. Phys.* **1985,** *82,* 5742.
(64) Wyckoff, R. W. G. *Crystal Structures*, 2nd ed.; Wiley: New York, 1963; Vol. 1, p 10.
(65) Trömel, M.; Lupprich, E. *Z. Anorg. Chem.* **1975**, *414*, 160.
(66) Churchill, M. R.; Hutchinson, J. P. *Inorg. Chem.* **1978**, *17*, 3528.
(67) Kirlin, P. S.; van Zon, F. B. M.; Koningsberger, D. C.; Gates, B. C. *J. Phys. Chem.* **1990,** *94,* 8439.

results in the high-k range ($7.50 < k < 16.26$ Å^{-1}), as the metal−support contributions in this region are small. The EXAFS function calculated with the first-guess parameters was then subtracted from the overall EXAFS data, with the residual spectrum being expected to represent the Ir−support interactions. The difference file was estimated with two Ir−O contributions, Ir−O_s and Ir−O_l, as both short and long metal−support oxygen distances have been frequently observed.[53] The more accurate parameters were achieved by using the difference file technique, and the improved fits for the Ir−Ir, Ir−O_s, and Ir−O_l contributions were then added and compared with the raw data in both k space and r space; the fit was not yet satisfactory. The Fourier transform of the residual spectrum showed an additional contribution at r equal to about 1.5 Å, which was assumed to be an interaction between Ir and Al of the support. The structural parameters characterizing the Ir−Al contribution were determined by fitting the residual spectrum. The iteration was continued as stated above, until good overall agreement was achieved.

Analysis of EXAFS Data for Used Catalysts. The normalized EXAFS function for the used catalyst incorporating Ir_6 supported on γ-Al_2O_3 was obtained from the average of the X-ray absorption spectra from six scans. The data analysis was performed in k space over the range $3.69 < k < 14.99$ Å^{-1}, as well as in r space over the range $0 < r < 5$ Å, by using unweighted raw EXAFS data. The analysis procedure is the same as that for the fresh catalyst.

The analysis for the used catalyst incorporating the iridium aggregates was performed in k space over the range $3.67 < k < 15.60$ Å^{-1} and in r space over the range $0 < r < 5$ Å, by using the unweighted raw EXAFS data. The analysis procedure is the same as that for the fresh Ir_6/γ-Al_2O_3 catalyst, except that the second- and third-shell Ir−Ir contributions were included in the fit.

Conclusions

Surface-mediated synthesis was used to prepare $[Ir_6(CO)_{15}]^{2-}$ on γ-Al_2O_3 by treatment of adsorbed [Ir(CO)$_2$(acac)] in CO at 100 °C and 1 atm. The supported $[Ir_6(CO)_{15}]^{2-}$ was decarbonylated by treatment in He at 300 °C without a significant change in cluster nuclearity, giving Ir_6/γ-Al_2O_3. The supported Ir_6 clusters are nearly uniform and nearly molecular in character, being among the best defined supported metals. The supported Ir_6 clusters are stable catalysts for the hydrogenation of toluene at temperatures in the range of 60−100 °C; the turnover frequency at 60 °C with a toluene partial pressure of 50 Torr and a H_2 partial pressure of 710 Torr was 1.7×10^{-3} s^{-1}. EXAFS results characterizing the used catalyst show that the supported Ir_6 clusters remained intact during catalysis. The γ-Al_2O_3-supported Ir_6 catalyst is an order of magnitude less active (per total Ir atom) for toluene hydrogenation than a catalyst consisting of aggregates of iridium (with an Ir−Ir first-shell coordination number of 7.9, consisting of crystallites of about 50 atoms each, on average) supported on γ-Al_2O_3. Because toluene hydrogenation is known to be a structure-insensitive catalytic reaction, we suggest that the concept of structure insensitivity in catalysis may not extend to clusters as small as Ir_6. However, the reasons for the differences in catalytic activity of the Ir_6 clusters and the iridium aggregates are not understood; it may be that the difference in activity of the clusters and the aggregates does not represent an effect of cluster or aggregate size but instead represents an effect of the support as a ligand affecting the electronic state of the metal in the clusters more than that in the aggregates, which more nearly resemble bulk metallic iridium.

Acknowledgment. We thank A. D. Jones of the University of California at Davis for help with the mass spectrometry. This research was supported by the National Science Foundation (Grant No. CTS-9315340). We acknowledge beam time and the support of the U.S. Department of Energy, Division of Materials Sciences, under Contract No. DE-FG05-89ER45384, for its role in the operation and development of beam line X-11A at the National Synchrotron Light Source. The NSLS is supported by the Department of Energy, Division of Materials Sciences and Division of Chemical Sciences, under Contract No. DE-AC02-76CH00016. We are grateful to the staff of beam line X-11A for their assistance. We also acknowledge the Stanford Synchrotron Radiation Laboratory for access to beam time. The EXAFS data were analyzed with the XDAP software developed by Vaarkamp et al.[19]

JA952996X